Immunohistochemical Study on Wound Healing of a Muscle Flap Transferred into the Oral Cavity of Rats

Takayoshi Tobita, Tsugio Inokuchi

Second Department of Oral and Maxillofacial Surgery, Nagasaki University School of Dentistry

Tobita T and Inokuchi T. Immunohistochemical Study on Wound Healing of a Muscle Flap Transferred into the Oral Cavity of Rats. *Oral Med Pathol* 2001; 6: 29-36, ISSN 1342-0984.

The immunohistochemical expressions of FGF2, FGFR1, FGFR2, and their possible participation in the apoptosis of myofibroblast were studied in the healing process of a muscle flap transferred into the oral cavity of rats. At 14 days postoperatively, abundant myofibroblasts were observed in the early-granulating muscle flap, and at 18 days postoperatively, they began to gradually disappear. The FGF2 immunopositive area, the number of FGFR2-positive fibroblasts and TUNEL-positive fibroblasts reached a maximum at 18 days postoperatively and gradually decreased thereafter, and there was a significant correlation of expression between the FGFR2-positive fibroblast and TUNEL-positive fibroblast. On the other hand, FGFR1-positive fibroblasts were observed from day 10 to 21 in the granulation tissue formation of the muscle flap. These findings suggest that FGFR1 may participate as a factor affecting tissue remodeling of muscle flap healing, and that FGFR2 may play a role in programmed cell death or apoptosis of myofibroblast.

Key words: **contraction, myofibroblast, fibroblast growth factor-2, fibroblast growth factor receptor-1, fibroblast growth factor receptor-2**

Correspondence: **Takayoshi Tobita,** Second Department of Oral and Maxillofacial Surgery, Nagasaki University School of Dentistry, 1-7-1 Sakamoto, Nagasaki, 852-8588, Japan
Phone: +81-95-849-7704, Fax: +81-95-849-7705

Introduction

Myocutaneous flaps have been widely used for reconstruction of extensive oral mucosal defects after extirpation of oral cancers. Recently a muscle-only flap, which mucosalizes in the oral cavity, has been used for reconstruction of the oral mucosa (1-4). The disadvantage of this type of flap is that it undergoes significant contraction postoperatively. The reason for this phenomenon is not well-understood, but it has been demonstrated in a number of reports that myofibroblast, which has features of contractile fibers such as alpha smooth muscle actin (α-SMA), participates in flap contraction (5, 6) and that the disappearance of myofibroblast that occurs through apoptosis is responsible for wound contraction (7-9).

Growth factors have been shown to enhance apoptosis of myofibroblast (10, 11). In particular, FGF2 is a potent accelerating factor of wound healing, inducing apoptosis in myofibroblast (12). FGFs bind to specific cell surface receptors and cause an increase in cellular response. There are both high and low affinity receptors. While the low-affinity receptor, heparin sulfate proteoglycans, is required to bind FGFs to high-affinity receptors, four high-affinity receptors (FGFR1, FGFR2, FGFR3, and FGFR4) directly bind FGFs and transduce the proliferating signal to cell nuclei. Among these four receptors, FGFR1 and FGFR2 have been well studied. FGFR1 is detected in blood vessels, nerve cells and oligodendrocytes (13). FGFR2 is found in dermal fibroblasts and matured hepatocytes and thought to function mainly in cell maturation and maintenance of the differentiated state (14).

Although apoptosis of myofibroblast is reported to be additively increased by FGF2 during the wound healing process, it is not clear which type of FGF receptor participates with apoptosis of myofibroblast. The purpose of this study is to investigate the expressions of two FGF receptors, FGFR1 and FGFR2, and their possible participation in the apoptosis of myofibroblast during the healing process of a muscle flap transferred into the oral cavity of rats.

Materials and Methods

Animals

The animals used in this study were 31 eight-week-old male Sprague-Dawley rats weighing 300-350 g. The animals were housed in individual cages under standardized conditions of temperature and humidity and a light-controlled environment (12-hour light/dark cycle). They

were fed a standard diet and water *ad libitum*.

Surgical procedure

Twenty-four rats were used for the experimental group. Animals were anesthetized by an intraperitoneal injection of pentobarbital sodium (40 mg/kg body weight), and a skin incision was made along the midline of the neck.

The design of the sternomastoid muscle flap was based on microangiographical assessment of the vasculature. The occipital artery branching from the external carotid artery fed the sternomastoid muscle flap. The muscle flap was completely dissected from the surrounding muscle fascia and cut about 1 mm from the sternum. The lower two-thirds of the muscle was raised as a flap to preserve its mastoid pedicle and maintained in this position long enough to reach the oral defect without tension.

In the oral cavity, a muco-periosteum defect was made on the superior and buccal aspect of the mandible in the edentulous region. A longitudinal incision was made along the alveolar crest from the first molar to the anterior tooth and extended vertically across the lower lip to the inferior border of the mandible. The lip and the buccal flap were raised up to the mental foramen, leaving the periosteum. The periosteum was excised anteroposteriorly from the vertical incision to the mental foramen and superioinferiorly from the longitudinal incision to the lower border of the mandible. This resulted in a defect approximately 5 mm square (Fig. 1a).

The sternomastoid muscle flap was tunneled into the oral cavity to cover the muco-periosteum defect without tension and sutured to the surrounding oral mucosa with 5-0 absorbable polyglactin sutures (Fig. 1b). The skin incision was primarily closed and the buccal mucosa was sutured at the inferior border of the mandible to obtain a deep sulcus (Fig. 1c). Intravenous cephazolin sodium, 30 mg/kg, was administered for 4 days postoperatively.

For the seven control specimens (days 2, 7, 10, 14, 18, 21, and 28), the muco-periosteal flap was made on the edentulous region of the mandible. The pedicled portion of the muco-periosteal flap, about 5mm square, was dissected away from the alveolus to the inferior border of the mandible, in order to produce bone exposure similar to the experimental group. Finally, this flap was repositioned *in situ* and sutured to the surrounding mucosa (Fig 1d).

Light microscopic study

Animals were anesthetized (pentobarbital sodium, 40 mg/kg body weight) and then subjected to perfusion with buffered 4% paraformaldehyde for fixation at 2, 7 (n = 1 each), 10, 14, 18, 21, 28 (n = 4 each), 40 and 60 (n = 1 each) days after the operation. The flap site of the mandible was sliced at a thickness of about 5mm along the frontal plane using a diamond band saw. The sliced sections were decalcified in 10% EDTA at 4°C for two weeks, and embedded in paraffin. Tissue sections 4um in thickness were cut, mounted on silanizing slides, and stained with hematoxylin-eosin for optical-microscopic examination.

Antibodies

Affinity-purified rabbit polyclonal anti-human FGF2 (working dilution, 1:300), anti-human FGFR1 and R2 (working dilution, 1:200) antibodies were obtained from Santa Cruz Biotechnology (Santa Cruz Biotechnologies Inc., Santa Cruz, CA, USA). Mouse monoclonal antibody for anti-human α-SMA (working dilution, 1:400), which was used as a marker for myofibroblast, was obtained from the DAKO Japan (DAKO Japan Corp., Kyoto, Japan). Each antibody was diluted in PBS (pH 7.4).

Immunohistochemical procedure for FGF2, α-SMA, FGFR1 and FGFR2

After deparaffinization, sections to be stained for FGF2 were digested with 3 mg/ml bovine testis hyaluronidase (Type IV-S, 1010 U/mg; Sigma Chemical Corp., St. Louis, MO, USA) in PBS for 30 min at 37°C. Sections to be stained for FGFR1 and FGFR2 were digested with 0.1% trypsin (Type II-S, 1470 BAEE U/mg; Sigma Chemical Corp., St. Louis, MO, USA) in 0.05 M Tris-HCl, pH 7.6, containing 0.1% $CaCl_2$, for 5 min at room tempera-

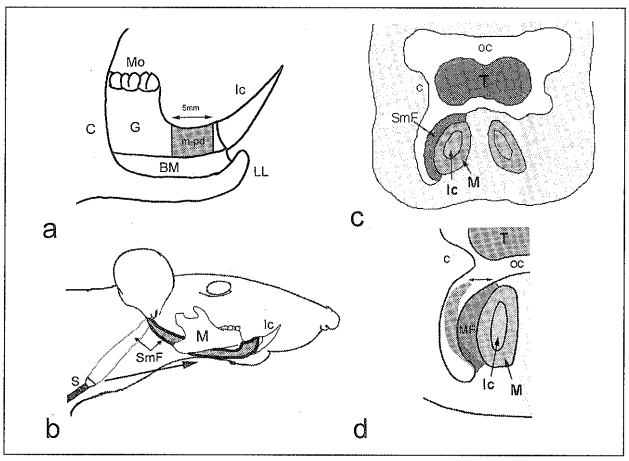

Fig. 1: (a) Design of the muco-periosteum defect (m-pd) in the edentulous region of mandible. Note that the defect region is 5 mm square.
(b) The sternomastoid muscle flap (SmF) transferred into the oral cavity. The flap was cut from the sternum, covered the muco-periosteum defect of the mandible, and sutured to the surrounding oral mucosa.
(c) Frontal section view of the flap covering the muco-periosteal bone defect.
(d) Frontal section view of the muco-periosteal flap (MF). Note that the flap was repositioned in situ after being dissected away from the mandible (double arrow).
BM = buccal mucosa, Mo = molar, Ic = incisor, G = gingiva, C = cheek, LL = lower lip, M = mandible, S = sternum, T = tongue, OC = oral cavity

ture. After washing in PBS, sections were treated with 3% H_2O_2 in methanol for 15 min to quench endogenous peroxidase. Treaded sections were incubated with 5% milk protein in PBS (FGF2, FGFR1 and FGFR2) for 30 min and 1.5% horse normal serum in PBS (α-SMA) to prevent non-specific protein binding and then with primary antibodies at 4°C overnight. The tissue sections were incubated with ENVISION+ (water soluble polymeric conjugates coupled to the peroxidase molecules and anti-rabbit antibodies, DAKO) and biotinylated horse anti-mouse IgG, followed by avidin-biotin peroxidase complex (Vector Laboratories, Inc., Burlingame, CA, USA). Finally, the sections were developed with 0.02% 3, 3'-diaminobenzide (Dohjindo, Kumamoto, Japan) in 50 mM Tris-HCl solution (pH 7.6) containing 0.006% H_2O_2 and counterstained with 1% methylgreen. As negative controls, the primary antibodies were replaced with PBS (pH 7.4) and either normal rabbit IgG (for FGF2, FGFR1, and FGFR2) or normal mouse IgG (for a-SMA).

TUNEL staining

Apoptotic cells were detected *in situ* by means of the terminal deoxynucleotidyle transferase (TdT)-mediated dUTP-biotin nick-end labeling (TUNEL) method (15), with the ApopTag system (INTERGEN Co., Purchase, NY, USA) according to the manufacturer's protocol. On sections used as negative controls for the specificity of labeling, distilled water was substituted for the TdT enzyme.

Quantitation of α-SMA, FGFR1, FGFR2, and TUNEL-positive fibroblasts

Histological sections for quantitation of a-SMA, FGFR1, and FGFR2 expression and apoptotic cells were obtained at 10, 14, 18, 21, and 28 days (n = 4 each) postoperatively. We calculated the percentage of positively stained fibroblasts by dividing the number of fibroblasts showing positive for anti-a-SMA antibody, anti-FGFR1 antibody, anti-FGFR2 antibody, and TUNEL by the total number of fibroblasts in 10 randomly selected different fields (total 0.625mm^2 per slide) at a magnification of 400× using an eyepiece graticule. a-SMA-, FGFR1- and FGFR2-positive cells were counted when a nucleus and at least one cytoplasmic process were present (16, 17).

Semi-quantitation of FGF2 with imaging analysis

FGF2-positive cells could not be quantitated because FGF2 widely stained not only cells but also the extracellular matrix in the granulation tissue. For this reason, we evaluated the percentage of FGF2-immunopositive area in the healing tissue of the muscle flap, using the image analysis program Scion Image Beta 4.02 Win (Scion Corp., Frederick, MD, USA) and a personal computer (Gateway Japan Inc., Tokyo, Japan). Histological sections for evaluation of the FGF2-immunopositive area were obtained at 10, 14, 18, 21, and 28 days (n = 4 each) postoperatively. Each section was photographed at three different fields in the center of the flap using a Nikon digital camera, COOLPIX 910 (Nikon Co., Tokyo, Japan), at a magnification of 200×. After saving the captured image in a personal computer, the image was cropped to a 256 × 256 pixel image. After noise reduction treatment and edge enhancement, image analysis was performed according to the method of Wu et al (18). The mean value of FGF2-immunopositive area was obtained from a total of 12 fields in four animals at each time point examined, and classified into four grades: + (obtained percentage of less than 10%), ++ (11% to 20%), +++ (21% to 30%), and ++++ (more than 31%).

Statistical analysis

Statistical analysis was performed using the Bartlett test. When the variance was comparable, one way analysis of variance (ANOVA) and Fisher's PLSD method for multiple comparisons were used to evaluate the staining patterns of the FGFR1-, FGFR2-, a-SMA-, and TUNEL-positive cells during the healing process of the flap. To study the correlation between expressions of FGFR2- and TUNEL-positive fibroblast, Pearson's correlation coefficient was used. p values less than 0.05 were considered to indicate statistical significance. However, the p value for Pearson's correlation coefficient was less than 0.001 The results were expressed as mean ± standard error.

Statistical analysis of each of the control groups from days 10 to 28 postoperatively was also performed by means of one way ANOVA and Fisher's PLSD method ($p<0.05$). However, no significant differences were observed and they can be regarded as a single group.

Results

Histopathological findings

On the 2nd postoperative day, the flap showed normal muscle striations and no necrosis. Acute inflammatory cell infiltration was seen at the periphery of the muscle flap on day 7. Granulation tissue was seen at the periphery of the muscle flap. The tip of the epithelium extending from the upper portion of the muscle flap was also observed (Fig. 2A). On days 10 and 14, the flap had been almost completely replaced by the granulation tissue with inflammatory cells infiltrating at the center of the flap. The surface of the granulating area, composed of immature connective tissues and numerous microvessels, was completely covered by the epithelium (Fig. 2B). By day 21, the granulation tissue had matured into fibrous tissue, and some inflammatory cells were still localizing at the center of the flap. Vessels of various sizes decreased in number by day 14 following the operation. On day 28, the flap was nearly replaced by fibrous tissue, while the periphery of the flap still contained some original musculature. The original buccal sulcus was reduced

Fig. 2: Histological features of the muscle flap.
(A) 7 days postoperatively (5×). Acute inflammatory cells (arrows) infiltrate the periphery of the flap.
(B) 14 days postoperatively (5×). Most of the flap is replaced by granulation tissue.
(C) 28 days postoperatively (5×). The flap is replaced by fibrous tissue (arrow). Buccal sulcus is obliterated and mobile cheek was retracted to the fibrous tissue of the flap by severe contraction.

by fibrous contraction in the flap area and the buccal mucosa was also retracted to the fibrous tissue of the flap as a result of severe contraction (Fig. 2C). On days 40 and 60 postoperatively, the original flap area was composed of fine collagen fibers and some fibroblasts. The contracted flap area consisted of hyperkeratinized epithelium and submucosal tissue composed of dense collagenous bundles parallel to the epithelium. There were few blood vessels in this contractile area.

On the other hand, many inflammatory cells were seen in the subepithelial region of the muco-periosteal flap on the 2nd postoperative day. After 7 days, the flap showed slight fibrous contraction, but no marked histopathological changes were observed in comparison with the experimental group (data not shown).

Immunohistochemical findings

(1) Myofibroblast

Myofibroblast was detected in the subepithelium at the adjacent mucosa of the muscle flap at 7 days postoperatively. At 14 days postoperatively, abundant myofibroblasts were observed in the early-granulating muscle flap (Fig. 3A), and intense expression of α-SMA was recognized in the cytoplasm of myofibroblasts (Fig. 3B). Immature small vessels were also seen. After 18 days postoperatively, the myofibroblast began to disappear, and at 28 days postoperatively, only small vessels were positive for α-SMA (Fig. 3C). Table 1 shows that the amount of myofibroblast reached a maximum at 14 days after the operation. Statistical analysis also revealed that, compared with day 14, there was a significant difference ($p < 0.05$) on days 10, 18, 21, and 28.

(2) FGF2

On the 7th postoperative day, FGF2-positive fibroblasts were occasionally seen in the subepithelium at the adjacent mucosa of the muscle flap. On days 10 and 14, morphological examination of the serial hematoxylin-eosin-stained sections resulted in the observation of migrating FGF2-positive macrophages at the granulating periphery of the muscle flap (Fig. 4A). At 18 days postoperatively, many FGF2-positive fibroblasts were observed in the granulation tissue (Fig. 4B). There was also a significant increase in the FGF2-positive area on day 18 as compared with days 10, 14, and 28 in the healing tissue of the muscle flap (Table 1). At 21 days postoperatively, the FGF2-positive fibroblasts were localized in the peripheral region rather than at the center of the flap. At 28 days postoperatively, FGF2-positive fibroblasts, being significantly reduced in number, were seen in the cicatricial fibrous tissue. After 21 days, the FGF2-positive area was also similar to the immunohistochemical findings (Table 1).

(3) FGFR1 and FGFR2

FGFR1-positive fibroblasts were observed from day 10 to 21 in the granulating tissue (Table1). Meanwhile,

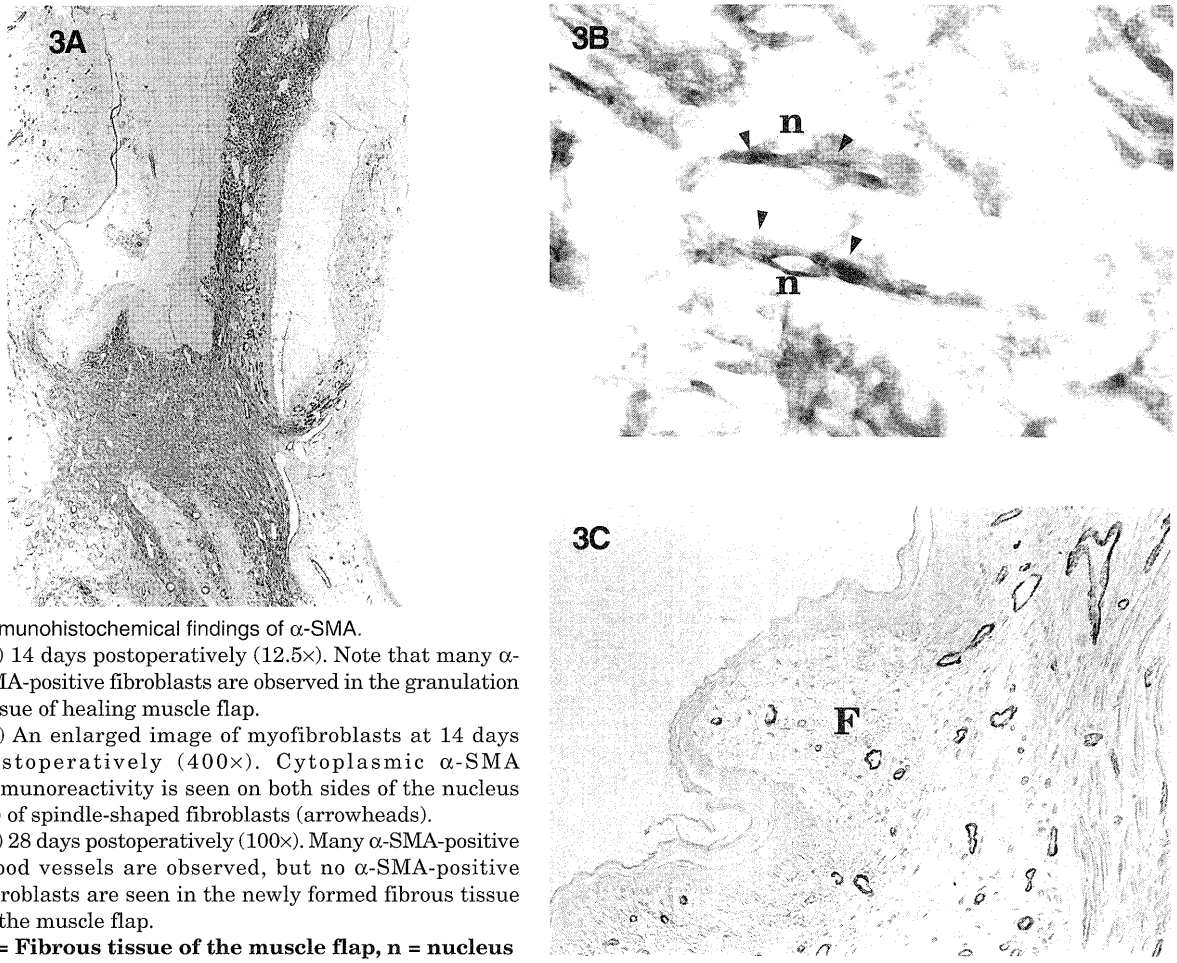

Fig. 3: Immunohistochemical findings of α-SMA.
(A) 14 days postoperatively (12.5×). Note that many α-SMA-positive fibroblasts are observed in the granulation tissue of healing muscle flap.
(B) An enlarged image of myofibroblasts at 14 days postoperatively (400×). Cytoplasmic α-SMA immunoreactivity is seen on both sides of the nucleus (n) of spindle-shaped fibroblasts (arrowheads).
(C) 28 days postoperatively (100×). Many α-SMA-positive blood vessels are observed, but no α-SMA-positive fibroblasts are seen in the newly formed fibrous tissue of the muscle flap.
F = Fibrous tissue of the muscle flap, n = nucleus

Table 1: **Evaluation of the FGF2 staining area, FGFR1-, FGFR2-, α-SMA-, and TUNEL-positive fibroblasts in the healing of the muscle flap.**

Days after operation	FGF2	α-SMA (% positive cells)	FGFR1 (% positive cells)	FGFR2 (% positive cells)	TUNEL (% positive cells)
Control	++	+ (1.23±0.93)	++ (12.26±2.43)	+ (7.82±0.99)	+ (5.53±2.55)
10	++	+++ (26.95±3.49)	++++ (35.15±3.21)	+ (5.40±2.68)	+ (6.17±2.03)
14	+++	++++ (41.96±6.64)*	+++ (29.74±2.27)	+ (4.27±1.44)	+ (2.77±0.76)
18	++++	+++ (27.66±2.84)	+++ (29.09±2.45)	+++ (26.39±8.47)**	++++ (43.81±9.71)†
21	+++	++ (16.34±4.74)	++++ (34.02±2.61)	++ (17.39±4.34)	+ (5.98±3.87)
28	++	+ (8.24±3.47)	++ (13.71±2.09)	+ (4.61±0.98)	+ (4.14±1.06)

We calculated the percentage of positive stained fibroblasts by anti-FGFR1 and FGFR2 antibody, anti- α -SMA antibody, and TUNEL for the total number of fibroblasts. The percentage of the FGF2 staining area was semi-quantitatively classified into four grades as: + (less than 10%), ++ (11% to 20%), +++ (21% to 30%), ++++ (more than 31%). Data is represented as mean±S.E.

*p<0.05 relative to day 10, 21, and 28 postoperatively.

**p<0.05 relative to day 10, 24, 21, and 28 postoperatively.

†p<0.05 relative to day 10, 24, 21, and 28 postoperatively.

FGFR2 was detected in the infiltrating inflammatory cells (mainly macrophages) on days 10 and 14 (Fig. 5A). On day 18, many fibroblasts, which include myofibroblast, were found to be FGFR2-positive in the granulation tissue (Fig. 5B). There was a significant difference in the FGFR2-positive ratios between day 18 and days 10, 14 and 28 ($p < 0.05$, Table 1). By day 21, FGFR2-positive fibroblasts decreased and were localized at the center of the flap. Thereafter, FGFR1 and FGFR2 gradually decreased in the fibrous tissue of the flap (Table 1).

(4) TUNEL-positive fibroblasts

TUNEL-positive cells were mostly fibroblasts, which were morphologically examined by means of HE-stained serial sections. At 14 days following the operation, TUNEL-positive fibroblasts were rarely seen in the granulation tissue of the muscle flap. At 18 days postoperatively, TUNEL-positive fibroblasts were observed throughout the flap area (Fig. 6A). Significant increases

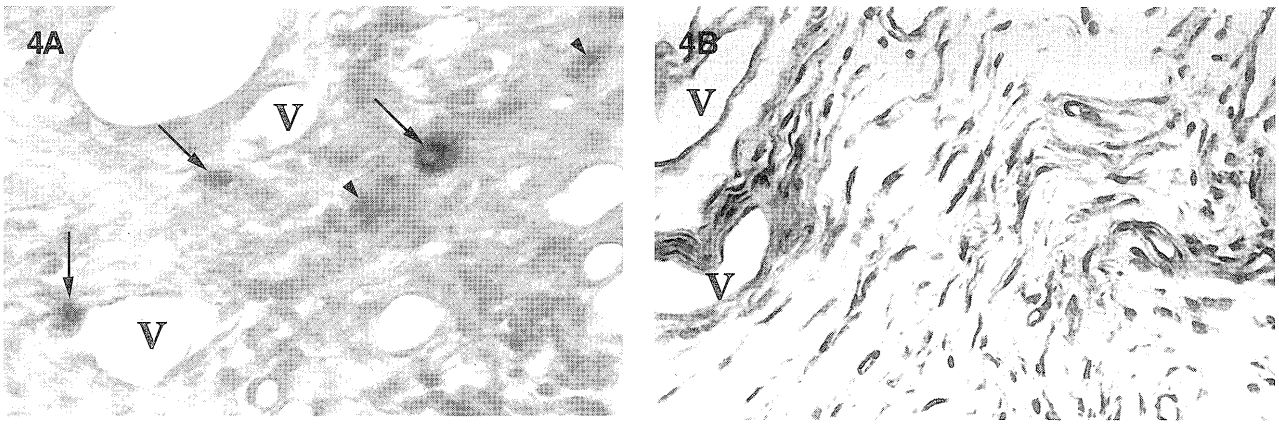

Fig. 4: Immunohistochemical findings of FGF2.
(A) FGF2-positive macrophages or monocytes (arrows) in the granulation tissue at 14 days postoperatively (400×). Many FGF2-positive fibroblasts were also observed in the granulating muscle flap, but stained weaker than FGF2-positive macrophages or monocytes (arrowheads). FGF2 granular immunoreactivity was also observed in extracellular matrices.
(B) 18 days postoperatively (200×). Note that FGF2-positive fibroblasts, having a spindle shape, are observed in the granulation tissue.
V = blood vessels

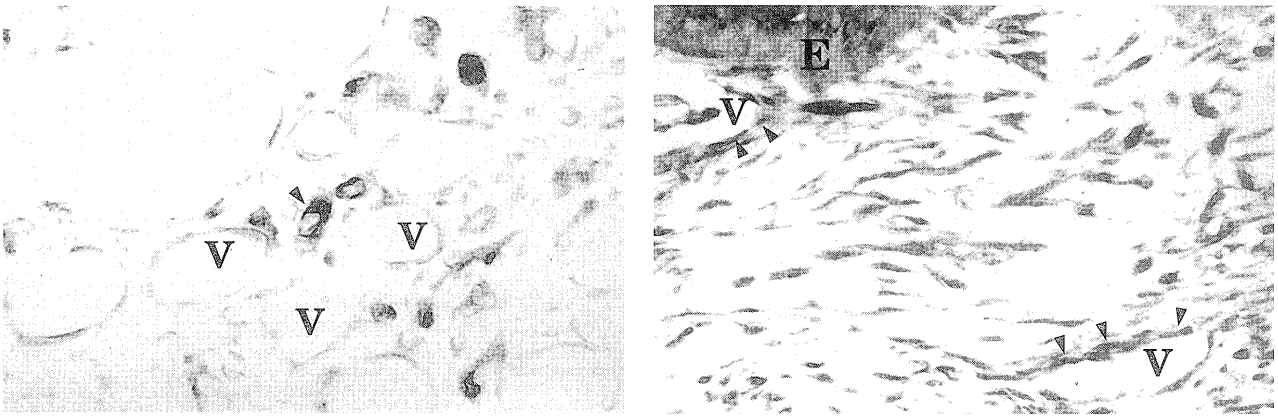

Fig. 5: Immunohistochemical findings of FGFR2.
(A) 14 days postoperatively (200×). FGFR2-positive macrophages or monocytes, having a round shape, are seen in the vicinity of the blood vessels (V) in the granulation tissue, and their immunoreactivity is mainly the cytoplasm of the cell (arrowheads).
(B) 18 days postoperatively (200×). Many FGFR2 immunopositive fibroblasts are observed in the granulation tissue. FGFR2-positive fibroblasts have a spindle shape, as do α-SMA-positive fibroblasts and FGF-2-positive fibroblasts. Some endothelial cells of the blood vessels were also seen (arrowheads) to be immunopositive.
E = Epithelium, V = blood vessels

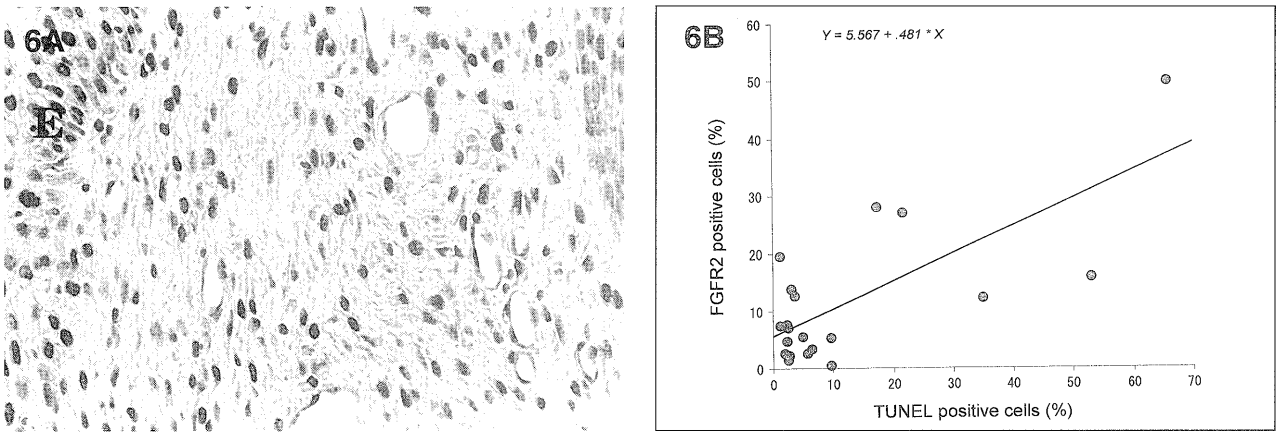

Fig. 6: (A) Histochemical findings of TUNEL staining at 18 day postoperatively.
TUNEL-positive fibroblasts are determined in the granulation tissue (200×).
E = Epithelium
(B) Correlation between expression of TUNEL-positive fibroblast and that of FGFR2-positive fibroblast.
Plot data represents the positive rate of TUNEL-positive fibroblast and FGFR2-positive fibroblast from day 10 to 28 postoperatively.
$r = 0.723$, $p < 0.001$

of TUNEL-positive fibroblasts were revealed between day 18 and days 10, 14, 21, and 28 ($p < 0.05$, Table 1). Regression analysis with the Pearson's correlation coefficient showed a highly significant correlation of expression between TUNEL-positive fibroblasts and FGFR2-positive fibroblasts ($r = 0.723$, $p < 0.001$, Fig. 6B). By day 21, TUNEL-positive fibroblasts were reduced in number, and by day 28, only a few TUNEL-positive fibroblasts were detected in the fibrous flap area.

Discussion

Wound healing features dynamic pathological events including inflammation, granulation, angiogenesis, fibrosis, epithelialization, and tissue remodeling (19). In the granulation stage, fibroblasts migrate from the periphery of the granulation tissue and secrete many extracellular matrices and growth factors. These factors accelerate tissue remodeling. Myofibroblast, which is a subtype of fibroblast and appears in the granulation stage, is interconnected by gap junctions and is connected to the extracellular matrices, such as fibronectin and collagen (20, 21). At first, wound contraction occurs when these cells start retraction (22). After epithelialization is completed, wound contraction occurs again, resulting in scar formation, and there is a striking decrease in cellularity. In particular, there is a disappearance of myofibroblast through apoptosis (8, 23). These events have also been observed in the healing process of the muscle flap in the oral cavity (5, 6).

In the present study, FGF2-positive macrophages were observed migrating to the granulating tissue of the muscle flap on day 14, when the amount of myofibroblast increased most substantially. Thereafter, the FGF2-positive area increased in the granulation tissue of the muscle flap (18 days postoperatively). These findings suggest that FGF2 is secreted by macrophages via a paracrine mechanism (24, 25) and predominates over fibroblasts in the healing muscle flap. Moreover, the amount of myofibroblast decreased and TUNEL-positive fibroblasts and the FGF2-positive area increased. We then suspected that most of the myofibroblasts might be included in TUNEL-positive cells, because certain reports have described that apoptotic fibroblasts increase when myofibroblasts decrease in number (7, 8). These observations are consistent with the study by Funato et al. reporting apoptosis of myofibroblast induced by FGF2 (11), suggesting that disappearance of myofibroblast results from apoptosis by FGF2.

FGF2, which is secreted from cells such as macrophages, endothelial cells and fibroblasts, binds to FGF receptors and transduces many cell growth signals (26-28). In these receptors, FGFR1 and FGFR2 have been well studied by many people. FGFR1 is mainly expressed in highly proliferative cells, such as tumor cells and embryonic mesenchymal cells (29), and is considered to be important for cell growth and activity (24). In this experiment, FGFR1-positive fibroblasts have been seen from 10 to 21 days postoperatively, corresponding to the granulating stage in the wound healing of the muscle flap. This result suggests that FGFR1 may play an important role in tissue remodeling in muscle flap healing.

On the other hand, FGFR2-positive fibroblasts increased with the increment of the FGF2-positive area, and the TUNEL-positive rate reached a maximum in our experiment. Moreover, the amount of myofibroblast continuously decreased in the granulating flap. Interestingly, the FGFR2-positive rate was nearly identical to the α-SMA-positive rate (Table 1), and there was a significant positive correlation between expression of FGFR2 and TUNEL in these fibroblasts (Fig. 6B).

FGFR2 regulates cell kinetics (14). Feng et al. reported that FGFR2 limits the tumorigenicity of prostate epithelial cells (30). This observation suggests that FGFR2 arrests cell growth, development, and differentiation. Cells that have finished biological activities including proliferation and differentiation, end the life span through apoptosis (31). The same phenomenon is observed in myofibroblast that is considered to be a terminally differentiated type of cell (8). Based on the above-noted reports and the results of our study, it is likely that FGFR2 plays a role for programmed cell death or apoptosis of myofibroblast. It is therefore a possibility that regulation of FGFR2 expression could be a clue to elucidate the pathological state, i.e., scarring and fibrotic contraction in tissue healing.

Various signal cascades of apoptosis have been elucidated through the present, but it is not evident if the signaling pathway from FGFR2 is involved in the apoptosis induction pathway. It is also possible that another growth factor may participate in the apoptosis of myofibroblast. However, it is possible that the downstream region of the apoptosis signal cascades overlap with the signaling pathway from FGFR2, or that another signaling pathway of FGFR2 exists in the upstream of the apoptosis signal cascades (32). Further investigation is needed to confirm the overlapping point between the signal transduction pathway of FGFR2 and the apoptosis-inducing pathway.

Acknowledgments

The authors would like to thank Dr. Natsuki Nagata, Institute for Medical Sciences, Kyoto University, and Dr. Yasuhisa Inoue, Department of Oral Histology, Nagasaki University School of Dentistry, for their helpful comments throughout the study; and Dr. Taku Toshima for his financial support.

References

1. Johnson MA, Langdon JD. Is skin necessary for intraoral reconstruction with myocutaneous flaps? *Br J Oral*

Maxillofac Surg 1990; **28**: 299-301.
2. Phillips JG, Postlethwaite K, Peckitt N. The pectoralis major muscle flap without skin in intra-oral reconstruction. *Br J Oral Maxillofac Surg* 1988; **26**: 479-85.
3. Inokuchi T, Uehara M, Yoshida S, *et al*. Use of the pectoralis major muscle-only flap for intraoral reconstruction. *Asian J Oral Maxillofac Surg* 1997; **9**: 27-30.
4. Ariyan S. The sternocleidomastoid myocutaneous flap. *Laryngoscope* 1980; **90**: 676-9.
5. Elshal EE, Inokuchi T, Sekine J, *et al*. Experimental study of epithelialization of the muscle-only flap in the oral cavity. *J Oral Maxillofac Surg* 1997; **55**: 1423-30.
6. Elshal EE, Inokuchi T, Yoshida S, *et al*. A comparative study of epithelialization of subcutaneous fascial flaps and muscle-only flaps in the oral cavity. A rabbit model. *Int J Oral Maxillofac Surg* 1998; **27**: 141-8.
7. Desmouliere A, Badid C, Bochaton Piallat ML, *et al*. Apoptosis during wound healing, fibrocontractive diseases and vascular wall injury. *Int J Biochem Cell Biol* 1997; **29**: 19-30.
8. Desmouliere A, Redard M, Darby I, *et al*. Apoptosis mediates the decrease in cellularity during the transition between granulation tissue and scar. *Am J Pathol* 1995; **146**: 56-66.
9. Desmouliere A. Factors influencing myofibroblast differentiation during wound healing and fibrosis. *Cell Biol Int* 1995; **19**: 471-6.
10. Funato N, Moriyama K, Baba Y, *et al*. Evidence for apoptosis induction in myofibroblasts during palatal mucoperiosteal repair. *J Dent Res* 1999; **78**: 1511-7.
11. Funato N, Moriyama K, Shimokawa H, *et al*. Basic fibroblast growth factor induces apoptosis in myofibroblastic cells isolated from rat palatal mucosa. *Biochem Biophys Res Commun* 1997; **240**: 21-6.
12. Khouw IM, van Wachem PB, Plantinga JA, *et al*. TGF-beta and bFGF affect the differentiation of proliferating porcine fibroblasts into myofibroblasts *in vitro*. *Biomaterials* 1999; **20**: 1815-22.
13. Wanaka A, Johnson EM Jr, Milbrandt J. Localization of FGF receptor mRNA in the adult rat central nervous system by *in situ* hybridization. *Neuron* 1990; **5**: 267-81.
14. Hu Z, Evarts RP, Fujio K, *et al*. Expression of fibroblast growth factor receptors flg and bek during hepatic ontogenesis and regeneration in the rat. *Cell Growth Differ* 1995; **6**: 1019-25.
15. Gavrieli Y, Sherman Y, Ben Sasson SA. Identification of programmed cell death *in situ* via specific labeling of nuclear DNA fragmentation. *J Cell Biol* 1992; **119**: 493-501.
16. Forbes JM, Leaker B, Hewitson TD, *et al*. Macrophage and myofibroblast involvement in ischemic acute renal failure is attenuated by endothelin receptor antagonists. *Kidney Int* 1999; **55**: 198-208.
17. Nakatsuji S, Yamate J, Kuwamura M, *et al*. *In vivo* responses of macrophages and myofibroblasts in the healing following isoproterenol-induced myocardial injury in rats. *Virchows Arch* 1997; **430**: 63-9.
18. Wu LC, D'Amelio F, Fox RA, *et al*. Light microscopic image analysis system to quantify immunoreactive terminal area apposed to nerve cells. *J Neurosci Methods* 1997; **74**: 89-96.
19. Moriyama K, Shimokawa H, Susami T, *et al*. Effects of growth factors on mucosal scar fibroblasts in culture--a possible role of growth factors in scar formation. *Matrix* 1991; **11**: 190-6.
20. Clark RA. Regulation of fibroplasia in cutaneous wound repair. *Am J Med Sci* 1993; **306**: 42-8.
21. Schmitt Graff A, Desmouliere A, Gabbiani G. Heterogeneity of myofibroblast phenotypic features: an example of fibroblastic cell plasticity. *Virchows Arch* 1994; **425**: 3-24.
22. Gabbiani G, Chaponnier C, Huttner I. Cytoplasmic filaments and gap junctions in epithelial cells and myofibroblasts during wound healing. *J Cell Biol* 1978; **76**: 561-8.
23. Desmouliere A, Gabbiani G. Modulation of fibroblastic cytoskeletal features during pathological situations: the role of extracellular matrix and cytokines. *Cell Motil Cytoskeleton* 1994; **29**: 195-203.
24. Myoken Y, Myoken Y, Okamoto T, *et al*. Immunohistochemical localization of fibroblast growth factor-1 (FGF-1), FGF-2 and fibroblast growth factor receptor-1 (FGFR-1) in pleomorphic adenoma of the salivary glands. *J Oral Pathol Med* 1997; **26**: 17-22.
25. Henke C, Marineili W, Jessurun J, *et al*. Macrophage production of basic fibroblast growth factor in the fibroproliferative disorder of alveolar fibrosis after lung injury. *Am J Pathol* 1993; **143**: 1189-99.
26. Murata M, Hara K, Saku T. Dynamic distribution of basic fibroblast growth factor during epulis formation: an immunohistochemical study in an enhanced healing process of the gingiva. *J Oral Pathol Med* 1997; **26**: 224-32.
27. Ledoux D, Gannoun Zaki L, Barritault D. Interactions of FGFs with target cells. *Prog Growth Factor Res* 1992; **4**: 107-20.
28. Coutts JC, Gallagher JT. Receptors for fibroblast growth factors. *Immunol Cell Biol* 1995; **73**: 584-9.
29. Dellacono FR, Spiro J, Eisma R, *et al*. Expression of basic fibroblast growth factor and its receptors by head and neck squamous carcinoma tumor and vascular endothelial cells. *Am J Surg* 1997; **174**: 540-4.
30. Feng S, Wang F, Matsubara A, *et al*. Fibroblast growth factor receptor 2 limits and receptor 1 accelerates tumorigenicity of prostate epithelial cells. *Cancer Res* 1997; **57**: 5369-78.
31. Warner HR. Aging and regulation of apoptosis. *Curr Top Cell Regul* 1997; **35**: 107-21.
32. Miyamoto T, Fox JC. Autocrine signaling through Ras prevents apoptosis in vascular smooth muscle cells *in vitro*. *J Biol Chem* 2000; **275**: 2825-30.

(Accepted for publication December 15, 2000)